

APPLICATION OF FLAC3D FOR SIMULATION OF THE BOREHOLE HYDRAULIC MINING OF NONG'AN OIL SHALE

GUI-JIE ZHAO, CHEN CHEN^{*}, XUE-JIAO DONG, FANG QIAN, WEI WANG, SHUAI GAO

College of Construction Engineering, Jilin University
Changchun 130026, P. R. China

***Abstract.** The analysis software, FLAC3D, was used for simulation of Nong'an oil shale mining according to the three-dimensional fast Lagrangian algorithm. A simulation study involving drilling hydraulic mining methods for different borehole spacings in the Nong'an oil shale mining area was conducted. The best mining scheme was selected in terms of safety factors and economic benefits, and used for the analysis of the vertical displacement and ground surface settlement of the oil shale area. Drill hole spacing was identified as a key factor for the coefficient of borehole hydraulic mining based on the general relationship between the coefficient and borehole spacing. The optimal mining hole spacing was 25 m, and the distribution regularities of the vertical displacement of the surrounding rock near the excavation and earth surface were observed. The results showed that FLAC3D can simulate and analyze the oil shale hydraulic mining process and is an effective and suitable method for oil shale exploitation research.*

***Keywords:** oil shale, simulation, borehole hydraulic mining, FLAC3D.*

1. Introduction

Oil shale is an unconventional oil and gas resource and is considered as a very important substitute for conventional energy resources in the 21st century because of its huge reserves and comprehensive utilization possibilities [1, 2]. Many countries, including China, are presently studying more recent oil shale mining methods. For example, researchers from Jilin University, China, have demonstrated the suitability of the borehole hydraulic mining method for extraction of deep-deposited oil shale [3, 4].

^{*} Corresponding author: e-mail chenchen@jlu.edu.cn

Borehole hydraulic mining is an emerging technology that differs from traditional underground tunnel mining and open-cast mining. The essence of this technology is the prior use of a high-pressure giant placed in the borehole to break the natural structure of solid seams or expand the cracks in the underground rocks. Then the rocks are crushed to form flowable slurry to be transported to the surface by using a water (gas) lifting device for further refinement. The basic principle of the technology was first proposed by the American scientist Aye-Kraay Thor already in 1932 and, independently, by the Russian investigator Tupicen in 1936 [5–14]. By borehole hydraulic mining only specialized workers are needed to operate the hydraulic mining drilling tools on the surface. The method is known to have many advantages, such as high mining depth, short building cycle, low investment in infrastructure, high safety, low labor intensity, and slight damage to the environment, specifically in mining areas where the oil rate is low and the depth of oil shale is great [15, 16]. The technique also has good application prospects [3].

Identifying a reasonable drilling spatial arrangement and maximum exploitation radius currently remains a problem to be solved in the borehole hydraulic mining of oil shale. The core problems are to determine a reasonable drilling interval and to maximize the coefficient of mining under the premise of surrounding rocks near the excavation stable, to provide safe mining equipment, and determine the ground surface settlement standard. In this study, the FLAC3D numerical analysis software was used to examine these problems under the actual geological conditions of the Nong'an oil shale mining area. The results are aimed to provide a reference for the borehole hydraulic mining of oil shale.

2. Principle of FLAC3D

2.1. Method of solution in FLAC3D

The method of solution in FLAC3D is characterized by the following three approaches:

- (1) finite difference approach in which first-order space and time derivatives of a variable are approximated by finite differences, assuming linear variations of the variable over finite space and time intervals, respectively;
- (2) discrete-model approach in which the continuous medium is replaced by a discrete equivalent – one in which all forces involved (applied and interactive) are concentrated at the nodes of a three-dimensional mesh used in the medium representation;
- (3) dynamic-solution approach in which the inertial terms in the equations of motion are used as numerical means to reach the equilibrium state of the system under consideration.

The laws of motion for the continuum are, by means of these approaches, transformed into discrete forms of Newton's law at the nodes. The resulting

system of ordinary differential equations is then solved numerically using an explicit finite difference approach in time.

The spatial derivatives involved in the derivation of the equivalent medium are those appearing in the definition of strain rates in term of velocities. For the purpose of defining velocity variations and corresponding space intervals, the medium is discretized into constant strain-rate elements of tetrahedral shape whose vertices are the nodes of the mesh mentioned above. A tetrahedron is represented in Figure 1 as an illustration.

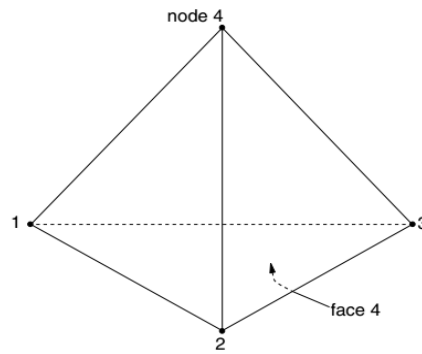


Fig. 1. Tetrahedron.

2.2. Finite difference approximation to space derivatives

The finite difference formulation of the strain-rate tensor components for the tetrahedron is derived below as a preliminary to the nodal formulation of the equations of motion. The tetrahedron nodes are referred to locally by a number from 1 to 4 and, by convention, face n is the opposite node n (Fig. 1).

By application of the Gauss divergence theorem to the tetrahedron, one can write:

$$\int_V v_{i,j} dV = \int_S v_i n_j dS, \quad (1)$$

where the integrals are taken over the volume and the surface of the tetrahedron, respectively, and n is the exterior unit vector normal to the surface.

For a constant strain-rate tetrahedron, the velocity field is linear, and n is constant over the surface of each face. Hence, after integration, Equation (1) yields:

$$V v_{i,j} = \sum_{f=1}^4 \bar{v}_i^{(f)} n_j^{(f)} S^{(f)}, \quad (2)$$

where the superscript (f) relates to the value of the associated variable on face f , and \bar{v}_i is the average value of the velocity component i . For a linear velocity variation, we have:

$$\bar{v}_i^{(f)} = \frac{1}{3} \sum_{l=1, l \neq f}^4 \bar{v}_i^{(l)}, \quad (3)$$

where the superscript (l) relates to the value at node l .

Substitution of Equation (3) in Equation (2) yields, reorganizing terms by node contribution:

$$V v_{i,j} = \frac{1}{3} \sum_{l=1}^4 \bar{v}^l \sum_{f=1, f \neq l}^4 \bar{v}_j^{(f)} S^{(f)}. \quad (4)$$

Replacing v_i by 1 in Equation (1) gives, by application of the divergence theorem:

$$\sum_{f=1}^4 n_j^{(f)} S^{(f)} = 0. \quad (5)$$

Using this relation and dividing Equation (4) by V , one can obtain:

$$v_{i,j} = \frac{1}{3V} \sum_{l=1}^4 v_j^l n_i^{(l)} S^{(l)}, \quad (6)$$

and the components of the strain-rate tensor may be expressed as:

$$\xi_{ij} = -\frac{1}{6V} \sum_{l=1}^4 (v_i^l n_j^{(l)} + v_j^l n_i^{(l)}) S^{(l)}. \quad (7)$$

FLAC3D can well analyze the dynamic process in which the formation and structure of strata in the oil shale mining area gradually stabilize until a plastic failure occurs. This process often happens in oil shale mining. FLAC3D can effectively simulate oil shale mining engineering [17, 18].

3. Simulation analysis

3.1. Geological conditions of the Nong'an oil shale mining area

Nong'an is rich in oil shale resources, which are distributed in a land area of over 400 km² and account for approximately 16.8 billion tons of industrial reserve. The mine area from the surface to the bottom comprises fine sand, clay, clay sand, sandstone, mudstone, sandstone, oil shale, and shale layers. All horizontal layers and their lithology, thickness, and mechanical parameters are given in Table 1. The oil shale layer is located 235 m to 240 m underground, and its thickness is 5 m. The average water level of this area is 6.06 m underground. In addition, a high tectonic compressive horizontal

stress is observed in the rocks. The tectonic stress changes linearly with depth, which can be calculated using the following formula:

$$\sigma = \alpha H + \beta, \quad (8)$$

where α is a gradient related to tectonic stress changing with depth (0.02 MPa/m), H is the depth from the surface, and β is the initial value of the tectonic stress (0.4808862 MPa).

The mining area layout is shown in Figure 2, in which circles denote the cylindrical excavations formed by borehole hydraulic mining, and A is the drilling interval.

Table 1. Physical and mechanical parameters of layers

Formation number	Lithology	Thickness, m	Density, kg·m ⁻³	Bulk modulus	Shear modulus	Friction, °	Cohesion, MPa	Tension, MPa
1	Fine sand layer	6.54	1470	6.67 MPa	5.0 MPa	28	–	–
2	Clay layer	6.81	1200	0.95 MPa	0.87 MPa	20	0.01	–
3	Loamy sand layer	5.10	1840	66.67 MPa	14.29 MPa	32	–	–
4	Sandstone layer	25.15	1880	37.5 MPa	17.31 MPa	32	–	–
5	Mudstone layer	78.23	2320	15.6 GPa	10.8 GPa	32.1	25	1.78
6	Sandstone layer	12.60	2170	26.8 GPa	7.0 GPa	27.8	27.2	1.17
7	Shale layer	100.57	2400	9.2 GPa	4.5 GPa	14.8	38.4	1.17
8	Oil shale layer	5.00	2000	8.8 GPa	4.3 GPa	14	29.3	0.96
9	Shale layer	60.00	2400	9.2 GPa	4.5 GPa	14.8	38.4	1.17

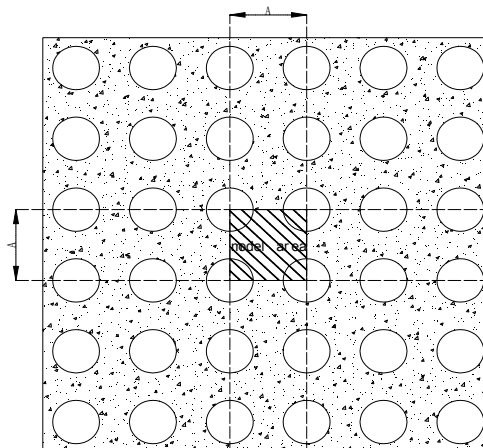


Fig. 2. Mining area layout.

3.2. The optimal mining scheme

The drilling interval can affect the coefficient of mining. Therefore, the following first seven drill hole spacing schemes should be compared and analyzed: Scheme 1 ($A = 10$ m), Scheme 2 ($A = 15$ m), Scheme 3 ($A = 20$ m), Scheme 4 ($A = 25$ m), Scheme 5 ($A = 30$ m), Scheme 6 ($A = 35$ m), and Scheme 7 ($A = 40$ m).

With the simulation process using Scheme 4, for example, a numerical model (length and width 25 m each and height 250 m) is initially generated (Figs. 3 and 4). The elastic constitutive model is used to generate an initial stress field. After completion, the constitutive model is changed into the Mohr-Coulomb model, and then the quarter-cylindrical shape step "exploitations" are conducted at the four corner points of the oil shale layer. The mining radius is increased by 1 m. Calculations are performed after each "exploitation" until the plastic zones appear, which indicates the occurrence of a plastic failure. During excavations the stability of the surrounding rock near the excavation and the safety of the mining equipment may be jeopardized. Thus, the actual mining radius should be smaller than the mining radius to ensure safety. However, a small mining radius cannot increase the economic benefit from oil shale mining. Therefore, the maximum radius r_{\max} should be equal to the radius value before entering the first plastic zone. No plastic zone appeared in the model when excavations were performed in step 7 (mining radius 7 m), as shown in Figure 3. However, plastic zones appeared when excavation was performed in step 8, as shown in Figure 4. Thus, r_{\max} in this scheme should be 8 m.

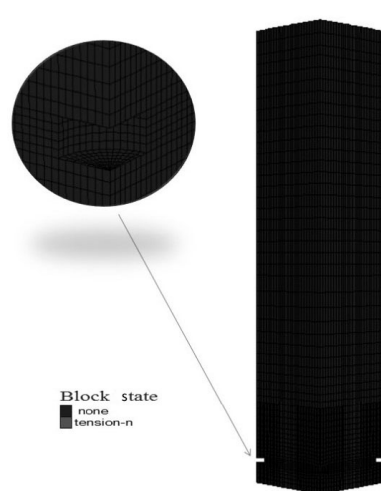


Fig. 3. Plastic zone map (mining radius 7 m).

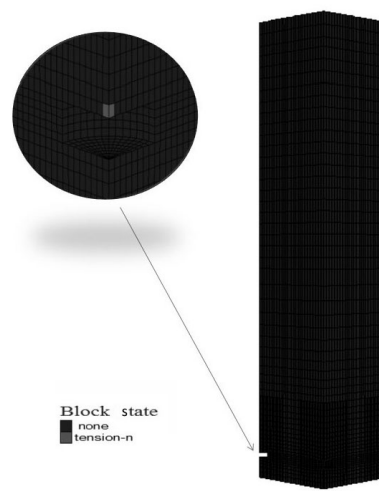


Fig. 4. Plastic zone map (mining radius 8 m).

Analysis of simulation schemes 1 to 7 yielded r_{\max} in different programs and allowed the calculation of the coefficient of oil shale mining under different schemes. Data are shown in Table 2 and Figure 5.

Table 2. r_{\max} in different programs

Program	1	2	3	4	5	6	7
A/m	10	15	20	25	30	35	40
r_{\max}/m	2	4	5	7	7	7	7

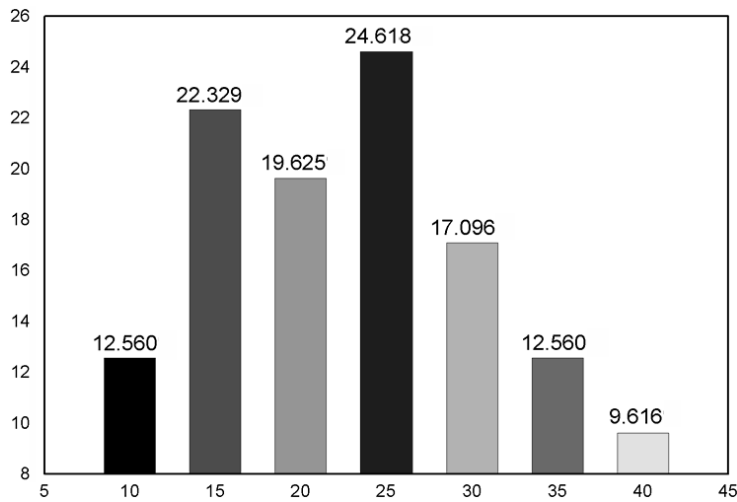


Fig. 5. Histogram of exploiting rate changes, %.

When the drilling interval changed, r_{\max} and the coefficient of mining also changed. Table 2 shows that r_{\max} increases with increasing A when A is smaller than 25 m. When A is larger than 25 m, r_{\max} remains constant and is not affected by A. Figure 5 shows that when A is equal to 25 m, Scheme 4 is selected, and the coefficient of mining of this mine lot can be maximized. Thus, when actual excavations are conducted, Scheme 4 and $r_{\max} = 7$ m are suitable.

3.3. Analysis of the vertical displacement of mining

After the exploitation of the underground ore body, the equilibrium state of the original rock stress is destroyed, resulting in the mobile deformation of the upper formation or destruction of the cave [19, 20]. Thus, the displacement field of surrounding rocks near the excavation should be known. Based on the analysis of the Scheme 4 model, a contour map of vertical displacement is obtained when the mining radius was 7 m, as shown in Figure 6. A vertical slice was generated along the diagonal direction of the model top, as shown in Figure 7.

After exploitation, a new displacement field was generated in the model. Figures 6 and 7 depict large vertical displacements in the roof and floor of each mined-out area. The directions of these displacements all point internally, and the displacement in the middle of each mined-out area is the largest and is decreasing. The displacement of the nonexcavated rock mass is very small.

Monitoring of the node displacements in the roof and floor of the mined-out areas enabled the construction of a graph of the vertical displacement $zdis$ against the distance from the node to the central axis of the mined-out area, as shown in Figures 8 and 9.

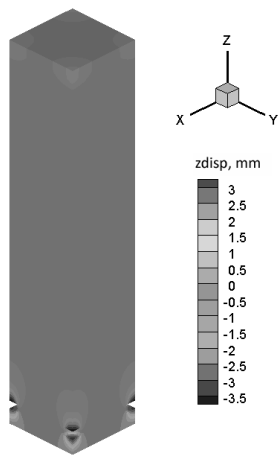


Fig. 6. Contour map of vertical displacement after exploitation.

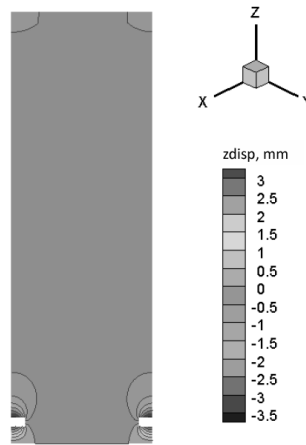


Fig. 7. Contour map of vertical displacement on the slice.

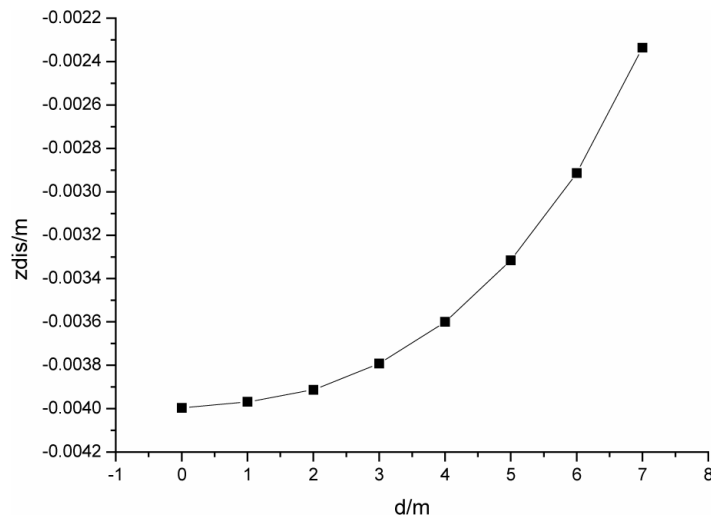


Fig. 8. Vertical displacement of roof grids.

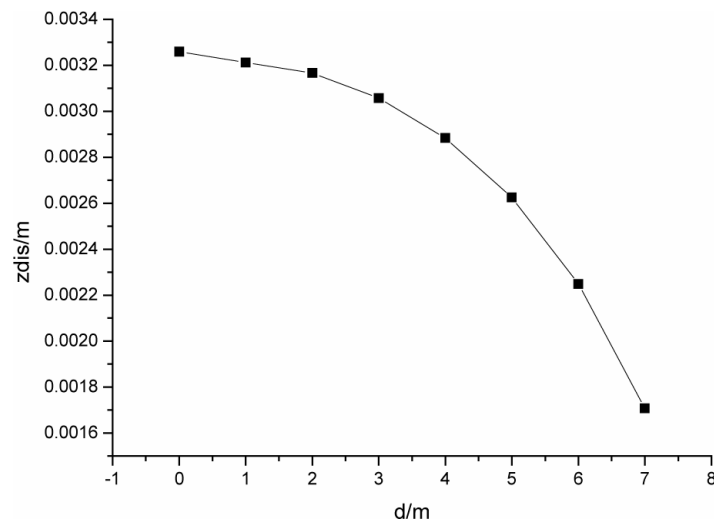


Fig. 9. Vertical displacement of floor grids.

The nodes in the roof and floor of the mined-out areas produced vertical displacements, resulting in deformation in the mined-out area. Figures 8 and 9 show that the shape of the roof after vertical displacement is concave upward, the floor is convex upward, and the vertical displacement of the roof is larger than that of the floor.

3.4. Analysis of the surface settlement

Excavation of underground rock and soil can cause surface subsidence and deformation. When surface subsidence increases to a certain extent, the safety of the construction on the ground is affected [21]. By monitoring node displacements on the surface, a graph of the surface subsidence $zdis$ against the distance from the node to the central axis of the mined-out area is obtained, as depicted in Figure 10.

Surface settlement appears after the exploitation of oil shale, and the value of the settlement is related to the distance (d) from the node to the central axis. Figure 10 also shows that the most serious surface settlement appears at the upright top position. The settlement becomes smaller as d increases. The settlement of this mining lot is small, hence producing no effect.

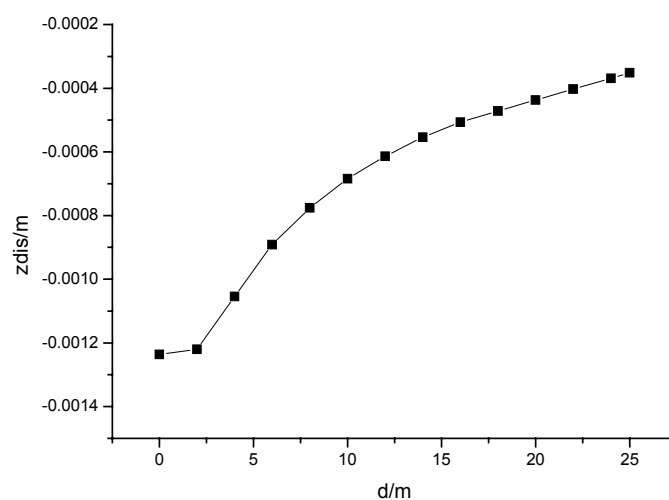


Fig. 10. Surface settlement.

4. Conclusions

- 1) The FLAC3D, developed according to the principle of three-dimensional fast Lagrangian analysis, demonstrated its ability to reasonably simulate the yield or plastic flow characteristics of rock mass in the actual process of production in the Nong'an oil shale borehole hydraulic mining area. FLAC3D also plays a significant role in simulating underground excavation and analyzes well yield failure and the settlement of displacement.
- 2) By FLAC3D simulation, the highest coefficient of oil shale hydraulic mining in Nong'an was estimated to be around 25%, which is quite a low value. Drilling hydraulic mining should be developed to improve the extraction rate of oil shale.
- 3) This study applied the three-dimensional fast Lagrangian method to the oil shale borehole hydraulic mining project design, and the research results provided a reference basis for shale borehole hydraulic mining.

REFERENCES

1. Zhao-jun Liu, Rong Liu. Oil shale resource state and evaluating system. *Earth Science Frontiers*, 2005(3), 315–323 (in Chinese).
2. Li Shuyuan, Tang Xun, He Jilai, Qian Jialin. Global oil shale development and utilization today – Two Oil Shale Symposiums held in 2012. *Sino-Global Energy*, 2013(1), 3–11 (in Chinese).
3. Da-yong Chen. *Research on Experimental Table of Nozzle Performance Test for Borehole Hydraulic Mining and Cylindrical Nozzle Optimization*. Dissertation, Jilin University, 2012 (in Chinese).

4. Yan He. *Research and Development of Experiment Platform for Borehole Hydraulic Mining of Oil Shale*. Dissertation, Jilin University, 2011 (in Chinese).
5. Liljegren, L. M., Bamberger, J. A. Pneumatic conveying of wet and dry solids through a vertical pipe. *American Society of Mechanical Engineers Fluids Engineering*, 1995, **228**(1), 401–408.
6. Zhong-hou Shen, Gen-sheng Li, Zhi-ming Wang, Xu Yiji. New jet theory and prospects of its application in drilling engineering. *Proceedings of the 13th World Petroleum Congress*, Buenos Aires, 20–25 October 1991, Argentina, 1991, 397–405.
7. Fu Chun, Yan En-feng. New mining technique – bore hydromining. *Mining and Metallurgical Engineering*, 2004(8), 7–8 (in Chinese).
8. Chen Chen. Drilling hole hydraulic mining – a new method of the mining technology. *World Geology*, 1998(12), 85–87 (in Chinese).
9. Yang Lin, Tang Chuan-lin, Zhang Feng-hua. The technology of hydraulic borehole for underground mining and its application. *Chinese Journal of Underground Space and Engineering*, 2006(4), 662–665 (in Chinese).
10. Gen-sheng Li, Jia-ji Ma, Xiao-ming Shen et al. A study on mechanisms and effects of plug removal near wellbore with high pressure water jet. *Acta Petrolei Sinica*, 1998, **19**(1), 96–99 (in Chinese).
11. Gen-sheng Li, De-bing Zhang et al. Mechanisms and experiments of self-excited pulsating water-injection. *Acta Petrolei Sinica*, 2002, **23**(6), 95–98 (in Chinese).
12. Yong-yin Yang, Zhong-hou Shen, Rui-he Wang et al. Experimental studies on radial horizontal drilling technology. *Petroleum Drilling Techniques*, 1998, **26**(1), 4–8 (in Chinese).
13. Obara, T., Bourne, N. K., Field, J. E. Liquid-jet impact on liquid and solid surfaces. *Wear*, 1995, **186–187**(Part 2), 388–394.
14. Chen Chen, Zu-pei Zhang. Borehole hydromining. *China Mining Magazine*, 1998(6), 40–43 (in Chinese).
15. Zhang Jian-yuan. Predict the future development of mining technology. *Foreign Metal Mining Magazine*, 1990(5), 2–9 (in Chinese).
16. Qiefu, B., Nikolaev, A. H. Deep hydraulic mining technology – a new method of mineral resources exploitation. *Foreign Metal Mining Magazine*, 1995(12), 33–40 (in Chinese).
17. Yu-min Chen, Ding-ping Xu. *FLAC/FLAC3D Basic and Projects*. Beijing: China Water Power Press, 2009, 94 (in Chinese).
18. Wen-bing Peng. *FLAC3D Practical Tutorial*. Beijing: China Machine Press, 2007, 1–2 (in Chinese).
19. Guo-quan Sun, Juan Li, Xing-bao Hu. FLAC3D-based stability analysis of mined-out area. *Metal Mine*, 2007(2), 29–32 (in Chinese).
20. Liu Yu-cheng. Study on FLAC3D simulation of surface ground movement process for underground seam mining. *Coal Science and Technology*, 2012(5), 93–95 (in Chinese).
21. Ming-zhou Bai, Zhao-yi Xu, Aijun Zhang, Jun Lei, Jin-shui Xie. Analysis of ground settlement of a subway station undercut with shallow overburden during construction with FLAC3D under complex geological conditions. *Chinese Journal of Rock Mechanics and Engineering*, 2006(10), 4254–4260 (in Chinese).

Presented by E. Reinsalu

Received June 7, 2013